

# Gold Nanoparticle-Functionalized Thread as a Substrate for SERS Study of Analytes Both Bound and Unbound to Gold

David R. Ballerini, Ying H. Ngo, Gil Garnier, Bradley P. Ladewig, and Wei Shen

Dept. of Chemical Engineering, Monash University, Clayton, Victoria 3800, Australia

Purim Jarujamrus

Dept. of Chemical Engineering, Monash University, Clayton, Victoria 3800, Australia

Dept. of Chemistry, Faculty of Science, Ubon Ratchathani University, Varinchamrap, Ubon Ratchathani 34190, Thailand

DOI 10.1002/aic.14398

Published online February 18, 2014 in Wiley Online Library (wileyonlinelibrary.com)

*The potential of thread for use as a substrate for inexpensive, disposable diagnostics for surface-enhanced Raman scattering (SERS) spectroscopy has been showed in this study. Gold-nanoparticle coated thread can be embedded into fabrics to detect chemical or biological analytes in military and medical applications through SERS. Using this inexpensive and widely available material enables reduction in the volumes of nanoparticle solution required compared to alternatives. By testing multiple analytes, it was observed that molecular structure played a significant role in SERS signal amplification, and hence, the technique is limited to the detection of a small number of analytes possessing highly polarizable structures. Although direct chemical bonding between analyte molecules and nanoparticles gives the strongest signal enhancement, it remains possible to easily discern signals generated by analytes not directly bound, provided they possess suitable structure. Amplification of SERS signal by controlling the aggregation state of the gold nanoparticles to increase the number of SERS hotspots was observed. © 2014 American Institute of Chemical Engineers AIChE J, 60: 1598–1605, 2014*

*Keywords: thread-based diagnostics, surface-enhanced Raman scattering, Raman enhancement, gold nanoparticles, unbound molecules*

## Introduction

Surface-enhanced Raman scattering (SERS) using metallic nanoparticles is a prominent technique for detecting and analyzing the adsorption of target molecules on substrates, and allowing different orientations and interactions of the molecules with the substrate to be determined. A highly SERS-active substrate is the most important factor in producing efficient SERS analysis. Previously, aqueous metal nanoparticle suspension were used in most SERS techniques, but this limits the applications of SERS as the specimens analyzed must be water soluble. To overcome this limitation and enhance the SERS technique, solid and rough SERS-active surfaces such as silicon wafers,<sup>1–3</sup> nanorod arrays on glass,<sup>4</sup> metal island films formed through thermal evaporation,<sup>5,6</sup> and laser ablated metal plates<sup>7</sup> were explored among others. However, these methods involve complex preparation of substrates and sophisticated instrumentation, thus, resulting in high costs which limit the applications of SERS. Therefore, the development of low cost, efficient, reliable, and reproducible SERS substrates is imperative.

Performing SERS with metallic nanoparticles coated low-cost substrate, such as filter paper, has been reported<sup>8</sup>; the use of paper as a substrate eliminates the need for the analytes examined to be water soluble, offering a much simpler method. The intertwined structure of cellulose fibers in paper was found to be able to “freeze” the adsorption state of nanoparticles by rapidly drawing away the water upon drying, resulting in a uniform distribution of gold nanoparticle (AuNPs) on paper, which is an important criteria for higher SERS reproducibility.<sup>8,9</sup> Besides that, adsorption of nanoparticles on the three-dimensional (3-D) multilayer cellulose structure of paper allows interlayer and intralayer plasmon coupling which is able to amplify the SERS signal<sup>10</sup>

Having similar cellulose structure as paper, thread can also be used as a highly SERS-active substrate. This work demonstrates the first use of thread as a low cost SERS substrate. Thread is inexpensive and globally ubiquitous. It possesses excellent color display properties, physical strength, and wettability. Thread is able to wick liquids through capillary action due to its porous structure formed by the spaces between the thread’s fibers.<sup>11–13</sup> This study used cotton thread exclusively, an ancient material used for centuries which is also an attractive substrate for the fabrication of low cost and low volume devices for SERS.<sup>14</sup> To the best of our knowledge, no work has reported using cotton or other multifilament threads for fabricating simple and low-cost substrates for SERS applications to date.

Correspondence concerning this article should be addressed to W. Shen at wei.shen@monash.edu.

\*David R. Ballerini and Ying H. Ngo contributed equally as co-first authors.

This study demonstrates the potential of AuNP treated cotton thread as a powerful tool for studying the surface configuration of molecules in SERS applications. The natural, porous morphology and high oxygen density of the thread structure provides a strong capillary force to adsorb AuNP-solution, allowing the deposition of AuNPs over a higher surface area than other flat substrates such as glass or polymer. In addition, cotton thread is inexpensive and only a tiny volume of AuNPs deposited on cotton thread can produce a wide range of diagnostic devices which show excellent surface-enhanced Raman scattering (SERS) behavior. Cotton thread has the advantage of being biodegradable, biocompatible, and renewable, and its structural morphology and surface chemistry can be readily engineered. Unlike paper, thread can be used to form fabric, which can be incorporated into apparel, for instance military attire, which can potentially be used for detection of biological hazard or chemical warfare reagents.

In this work, we have explored the optimum conditions to produce SERS-active AuNPs treated cotton thread by studying effect of size, concentration, and aggregation state of AuNPs on the SERS activity of the thread. The application of AuNP-functionalized thread in analyzing different molecule structures through SERS was demonstrated. This study also investigated the impacts of analyte polarizability and nanoparticle binding on SERS signals, results which are no doubt applicable to other substrates apart from thread.

## Experimental Section

### Materials and instrumentation

Hydrogen tetrachloroaurate trihydrate ( $\text{HAuCl}_4 \cdot 3\text{H}_2\text{O}$ ), sodium citrate tribasic dihydrate ( $\text{Na}_3\text{C}_6\text{H}_5\text{O}_7 \cdot 2\text{H}_2\text{O}$ ) and 4-aminothiophenol (4-ATP), 1-Decanethiol (1-DT), L-Methionine (LM), and Phenolphthalein were purchased from Sigma-Aldrich. Ninhydrin reagent was provided by CSIRO, Clayton. Cationic polyacrylamide (CPAM) of high molecular weights ( $\sim 13$  M Da) and charge densities at 40% wt (F1, SnowFlake Cationics) was purchased from AQUA+TECH, Switzerland. Ultrapure water purified with a Millipore system (18 M $\Omega$  cm) and Absolute ethanol were used in all aqueous solutions and rinsing procedures. Precut 5 mm  $\times$  7 mm silicon wafers were purchased from ProSciTech as a solid support for SERS.

Cotton thread was kindly provided by the school of Fashion and Textiles, RMIT University, Melbourne, Australia. Natural cotton thread is not wettable by aqueous liquids due to the presence of naturally occurring waxes on the surface of fibers and within the fiber wall. As such, natural cotton thread needs to be dewaxed, or surface treated, to allow the wicking of aqueous liquid.<sup>11</sup> In this study, natural cotton thread was rendered hydrophilic by exposure to plasma in a vacuum plasma reactor (K1050X plasma asher (Quorum Emitech, UK)) for 1 min at an intensity of 50 W. The vacuum level for the treatment was  $6 \times 10^{-1}$  mbar.

The morphology of the AuNP-functionalized thread was observed via field emission scanning electron micrograph (FESEM) using a JEOL 7001 FEG system operating at 5 kV and 180 pA. The Zeta potential measurements of the AuNP in the suspension form were performed with a Zetasizer Nano ZS (Malvern Instruments) in a Folded Capillary cell (DTS1060) at 25°C. All Raman and SERS spectra were obtained in the air on a Renishaw Invia Raman microscope equipped with 300 mW 633 nm laser. Typically, the laser was set to 10% of maximum power. The laser beam was

positioned through a Leica imaging microscope objective lens (50 $\times$ ), whilst the instrument's wavenumber was calibrated with a silicon standard centred at 520.5  $\text{cm}^{-1}$  shift. Due to the smaller spot size of the laser compared with the large surface area of the samples, spectra were obtained at different points along the thread surfaces, and were the same shape, differing only in intensity. The average intensity (of five measurements) was presented as the final result.

## Methods

### Preparation of AuNPs

AuNPs were synthesized using 1 mM of hydrogen tetrachloroaurate,  $\text{HAuCl}_4 \cdot 3\text{H}_2\text{O}$ , and 1% aqueous sodium citrate according to the Turkevich method.<sup>15</sup> To synthesize a stock solution of larger AuNPs (approximately 40 nm in diameter), a modified version of the Turkevich method was performed using 0.65 mM  $\text{HAuCl}_4 \cdot 3\text{H}_2\text{O}$  and 0.5% aqueous sodium citrate. A 20-mL solution of 1 mM of aqueous hydrogen tetrachloroaurate was heated to 100°C. 2 mL of 1% aqueous sodium citrate was then added to the heated aqueous hydrogen tetrachloroaurate. The mixture was then stirred and heated until its color transitioned from pale yellow to pale blue, and then into a brilliant red on completion. The AuNPs solution obtained was then allowed to cool to room temperature and stored at 4°C. To obtain a concentrated AuNPs solution, the original AuNPs solutions were concentrated 10x by centrifugation at 6000 g for 20 min.

### The adsorption of AuNPs to cotton-thread substrate

CPAM is among the most extensively used cationic polyelectrolyte flocculants for liquid/solid separation, retention and drainage aids in papermaking and flotation aids.<sup>4,16</sup> To induce more adsorption and aggregation of AuNPs in an effort to promote SERS signal amplification, thread substrates were treated with CPAM to engineer their surface charge. A stock solution of CPAM was prepared on the day of experiment by diluting dry powder to 0.01% with Ultrapure water purified with a Millipore system (18 M $\Omega$  cm) and the dispersions were gently shaken for 1 h to facilitate the dissolution process. Plasma-treated cotton-thread substrates of 10 mm length were dipped into the CPAM solution for 1 h, rendering the thread cationic. The treated cotton threads were then rinsed with distilled water and left to air dry. The treated cotton threads were then soaked individually in solutions of AuNPs. After soaking, the AuNP-treated cotton threads were rinsed thoroughly with distilled water to remove loosely bound AuNPs, and then air dried.

### Preparation of Raman active cotton-thread substrates and silicon wafers

Solutions of different concentrations of 4-ATP, 1-DT, Ninhydrin reagent, and Phenolphthalein were prepared in ethanol, whereas LM was prepared in distilled water. The dried nanoparticle-deposited thread substrates (both untreated and pretreated with cationic polymers) were dipped into a solution of analyte molecules for 5 min. After thorough rinsing with MilliQ water and drying, they were subjected to Raman characterization.

Silicon wafers with dimensions of 10  $\times$  10 mm<sup>2</sup> were cleaned with "piranha" solution (mixture of sulfuric acid and hydrogen peroxide) and ultrasonicated before use. Silicon wafers were also treated in the vacuum plasma reactor for 1 min at an intensity of 50 W. The vacuum level for the

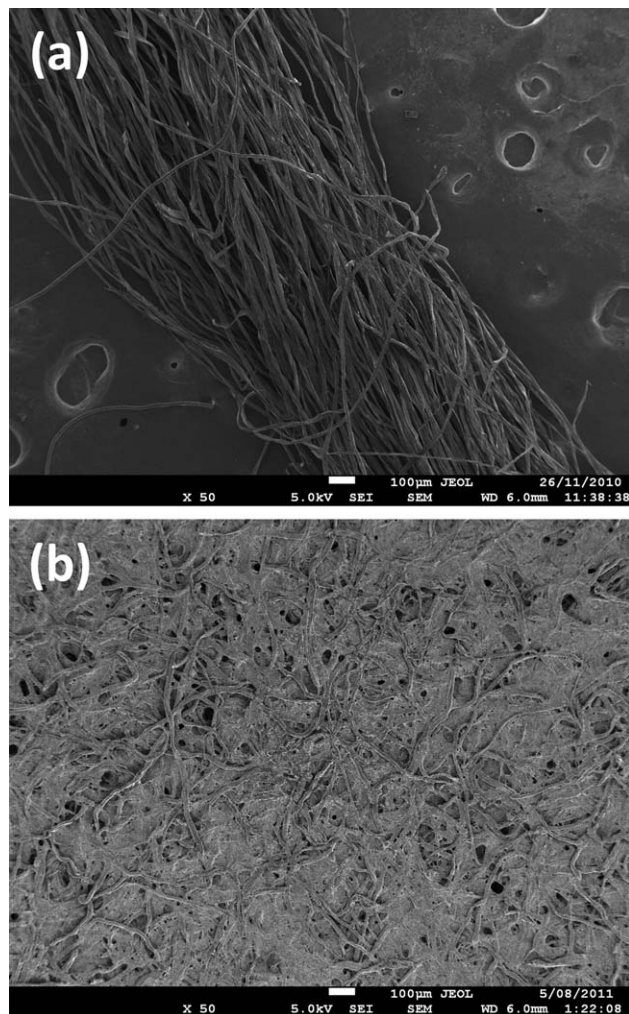


**Figure 1. FESEM images of (a) cotton thread and (b) filter paper.**

treatment was  $6 \times 10^{-1}$  m bar. 5  $\mu$ L of AuNPs was applied to each silicon wafer and dried in air before analysis.

## Results and Discussion

Cotton threads were analyzed under SEM to study their structure and morphology. It was found that cotton thread is composed of many cellulose fibers which are similar to those found in filter paper. However, the cellulose fibers of cotton thread (Figure 1a) are arranged in a twisted structure, as opposed to paper (Figure 1b) which has a layered cellulose fiber structure.

### Analyte testing

*Proof of Concept.* To assess the SERS potential of these AuNP-CPAM treated threads, the aromatic thiol known as 4-ATP (molecular structure shown in Figure 2b) was chosen as a probe molecule for the Raman analysis due to its distinct Raman features, strong affinity for metal surfaces, and formation of self-assembled monolayers.<sup>17</sup> Figure 2a shows the SERS spectra obtained from AuNPs-CPAM treated threads which were exposed to different concentrations of 4-ATP. Overall, the spectral features of 4-ATP are clearly shown, as opposed to the Raman spectrum of 4-ATP on untreated, plain thread. These spectra are dominated by six strong bands:  $\delta(\text{C—S})$  at 387  $\text{cm}^{-1}$ ,  $\nu(\text{C—S})$  at 1077  $\text{cm}^{-1}$ , and  $\nu(\text{C—C})$  at 1584  $\text{cm}^{-1}$  (in-

plane, in-phase modes) and  $\delta(\text{C—H})$  at 1137  $\text{cm}^{-1}$ ,  $\delta(\text{C—H}) + \nu(\text{C—C})$  at 1386  $\text{cm}^{-1}$ , and  $\delta(\text{C—H}) + \nu(\text{C—C})$  at 1433  $\text{cm}^{-1}$  (in-plane, out-of-phase modes) of the 4-ATP molecules.<sup>18</sup> By increasing the concentration of 4-ATP, the SERS intensity is increased accordingly and their characteristic peaks become more prominent (Figure 2a). The average intensity of the peak heights obtained using this technique were comparable to those achieved using a paper substrate under similar conditions,<sup>9</sup> albeit with greater variation between locations on the same thread, as shown in the calibration curve in Figure 2c. On one hand, this result suggests that a semiquantitative correlation may be established for concentration analysis of SERS active analytes, which is in qualitative agreement with our previous report for the paper-based SERS platform.<sup>8</sup> Conversely, the error bars (established by five repeat measurements) are quite large, much larger than those obtained from the paper-based SERS device.<sup>8</sup> The most likely reason for the more significant signal intensity variation on thread may be due to the fiber morphology in thread being so different from that in paper. While fibers in thread are not bound to one another and form a twisted helical bundle, those in paper bond to one another in a random crisscrossed fashion. Due to the small laser spot, the laser may only cover a small section of a substrate. As in different SERS measurements the laser hits different locations on the substrate, on a less compact fiber bundle of a thread the SERS signals show a greater variability.

Like conventional Raman spectrometry and Fourier Transform Infrared spectroscopy (FTIR), the advantage of SERS is more in the identification of qualitative information of the molecular structure through the enhancing effect of the hotspot, not in its quantitative value. This is because the signal intensity is strongly related to the matching of the electric field direction in the hotspot and the vibrational co-ordinate of the analyte. This in turn implies that the matching of incident laser polarization plane and orientation of hotspots is important.<sup>19</sup> Although it could be generally assumed that the distribution of AuNPs on a surface is random and the matching of the laser polarization plane with the orientation of hotspots would be relatively constant, for substrates that have grain structures such as thread, this assumption may not be reliable.

The most salient advantage of thread is the significant reduction in the volume of AuNP solution required to treat the substrate, due to the compact size and lower absorbency of the thread.<sup>17,20</sup> As the nanoparticles are composed of a precious metal it is desirable that their consumption should be limited as much as possible to reduce the cost-per-test. This effect also results in a reduction of the volume of sample required for testing, which may be useful in certain applications. The smaller thread substrate is also lighter and more robust, making it more suitable for transportation from the sample location to external testing facilities. There is also the possibility that testing threads could be mass-produced using a roll-to-roll format by separating the wettable testing zones via the application of hydrophobic reagents or other substances which block the porous structure of the thread (but are suitably SERS inactive). This result demonstrates the potential of thread to be developed as a SERS active substrate like paper for qualitative and semiquantitative analysis of analyte concentration.

### Parameters affecting SERS performance of AuNP treated thread

Following initial proof of concept studies, experiments were performed to determine if the size or concentration of

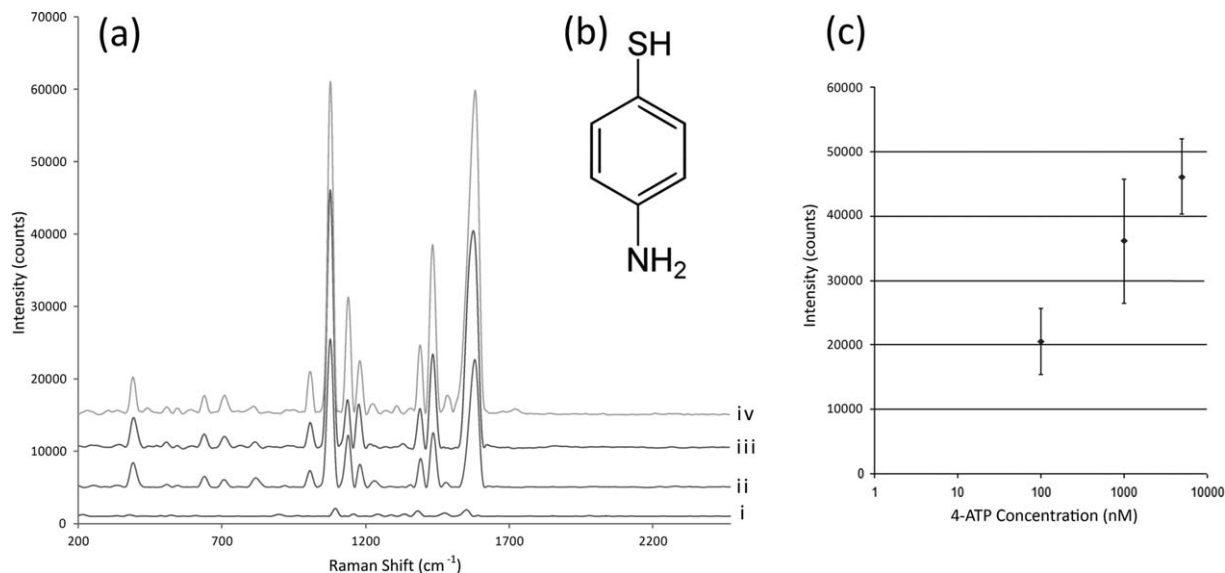


**Figure 2. (a) SERS spectra of 4-ATP at varying concentrations on both plain and CPAM treated threads.**

(1) Spectrum of 1 mM 4-ATP on plain thread, SERS spectra of, (2) 0.1 mM, (3) 1 mM, and (4) 5 mM of 4-ATP on AuNP-CPAM treated thread, (b) Molecular structure of the 4-ATP molecule, and (c) Calibration curve of the Raman intensity at the location of the  $1077\text{ cm}^{-1}$  peak, with bars showing the standard error over five repetitions.

the NPs played a role in the enhancement achieved during SERS. To determine the effect of NP size, threads were treated with AuNPs of different sizes: 20 and 40 nm. After soaking in the AuNP solution for 24 h, the color of the cotton thread changed from a cream white to dark purple/red as a result of the plasmon absorption of the AuNPs assembled on the substrates. The FESEM image shows that the adsorption of AuNPs is well dispersed on the surface of thread (Figures 3a and b). Figures 4b and c shows the SERS spectra obtained from threads which were treated with AuNPs of two different sizes and exposed to 1 mM of 4-ATP. Both SERS spectra clearly show the spectral features of 4-ATP, as opposed to the Raman spectrum of 4-ATP on untreated thread (Figure 9a), and are very similar in terms of their intensity.

To study the effect of AuNP concentration, the 20 nm AuNPs were concentrated using an ultracentrifuge (by 10 times). FESEM analysis (Figure 3c) showed that a higher surface coverage of AuNPs was achieved on the thread surfaces when the thread was treated with the concentrated AuNPs. Additionally, the SERS intensity increased and the characteristic peaks of the 4-ATP became more distinct (Figure 4d). This suggests that the concentration of AuNPs has more impact on the SERS signal enhancement compared to their size.

According to the literature, aggregates of nanoparticles have higher SERS efficiency than individual nanoparticles due to increased enhancement at the junctions between nanoparticles.<sup>21,22</sup> To amplify the SERS signal of the concentrated 20 nm AuNP treated thread, the aggregation of AuNPs was induced by pretreating the thread with 0.01% CPAM. This is able to produce a positive surface charge on cotton thread substrates and then promote the aggregation of the negatively charged AuNPs. As shown in Figure 3d, there was a significant increase in the adsorption and aggregation of AuNPs when the thread was pretreated by CPAM. The assembly of the AuNPs is brought into closer vicinity by forming a random distribution of 2-D and 3-D clusters, compared to the AuNP thread without CPAM (Figure 3c). As

AuNPs come in close contact when aggregated, their transition dipoles become coupled to each other and the enhanced fields of each nanoparticle start to coherently interfere at their contact point. Hence, their SERS signal is significantly enhanced (Figure 4e).

#### Effect of polarizability on SERS signal

In this study, 1-DT and LM were also selected to be studied. The purpose of selecting these two molecules was to evaluate the practical SERS effects on molecules with structures that are dominated by  $\sigma$ -bonds and localized valence electrons, and are also lacking of high level symmetry. As the surface enhanced Raman effect is proportional to the square of molecular polarizability change caused by changes in the vibrational co-ordinates of the molecule, highly localized valence electron structures would be less active to SERS. This study aims to provide an experimental evaluation to this point, which can be used as a practical guide for future SERS analysis. Threads were treated with 1-DT (Figure 5a) and LM (Figure 5b) to study their SERS properties. Interestingly, the SERS spectrum of 1-DT in Figure 6 does not show the characteristic peaks expected which are  $\delta(\text{C-H}_2)$  at  $1450\text{ cm}^{-1}$ ,  $\tau(\text{CH}_2)$  and  $\rho(\text{CH}_2)$  at  $1280\text{ cm}^{-1}$ ,  $\nu(\text{C-C})$  at  $1050\text{ cm}^{-1}$ ,  $\rho(\text{CH}_3)$  at  $880\text{ cm}^{-1}$ ,  $\tau(\text{CH}_2)$  and  $\rho(\text{CH}_2)$  at  $720\text{ cm}^{-1}$ , and  $\delta(\text{S-S-C})$  at  $370\text{ cm}^{-1}$ .<sup>23</sup> Besides that, the spectra are irreproducible and their intensity is similar to that of the blank AuNP-CPAM treated thread even though the concentration of 1-DT was increased up to 5 mM. The SERS spectrum of LM (spectra not shown) also follow the same trend as 1-DT; the characteristic peaks of  $\nu(\text{C}^4\text{-S})$  at  $680\text{ cm}^{-1}$ ,  $\nu(\text{C}^2\text{-C}^3)$  at  $860\text{ cm}^{-1}$ ,  $\nu(\text{C}^1\text{-C}^2)$  at  $945\text{ cm}^{-1}$ ,  $\nu(\text{C}^2\text{-N})$  at  $1040\text{ cm}^{-1}$ , and  $\nu_s(\text{COO}^-)$  at  $1400\text{ cm}^{-1}$ <sup>24</sup> are not visible and similar to the plain thread.

As there is no SERS signal coming from both 1-DT and LM on the AuNPs-CPAM treated threads, it is important to make sure these molecules are attached and reacted to AuNPs on the thread substrates. Therefore, 1 mM of 1-DT was mixed with AuNPs and dropped on silicon substrate. As observed on Figure 6, the SERS spectrum of 1-DT clearly

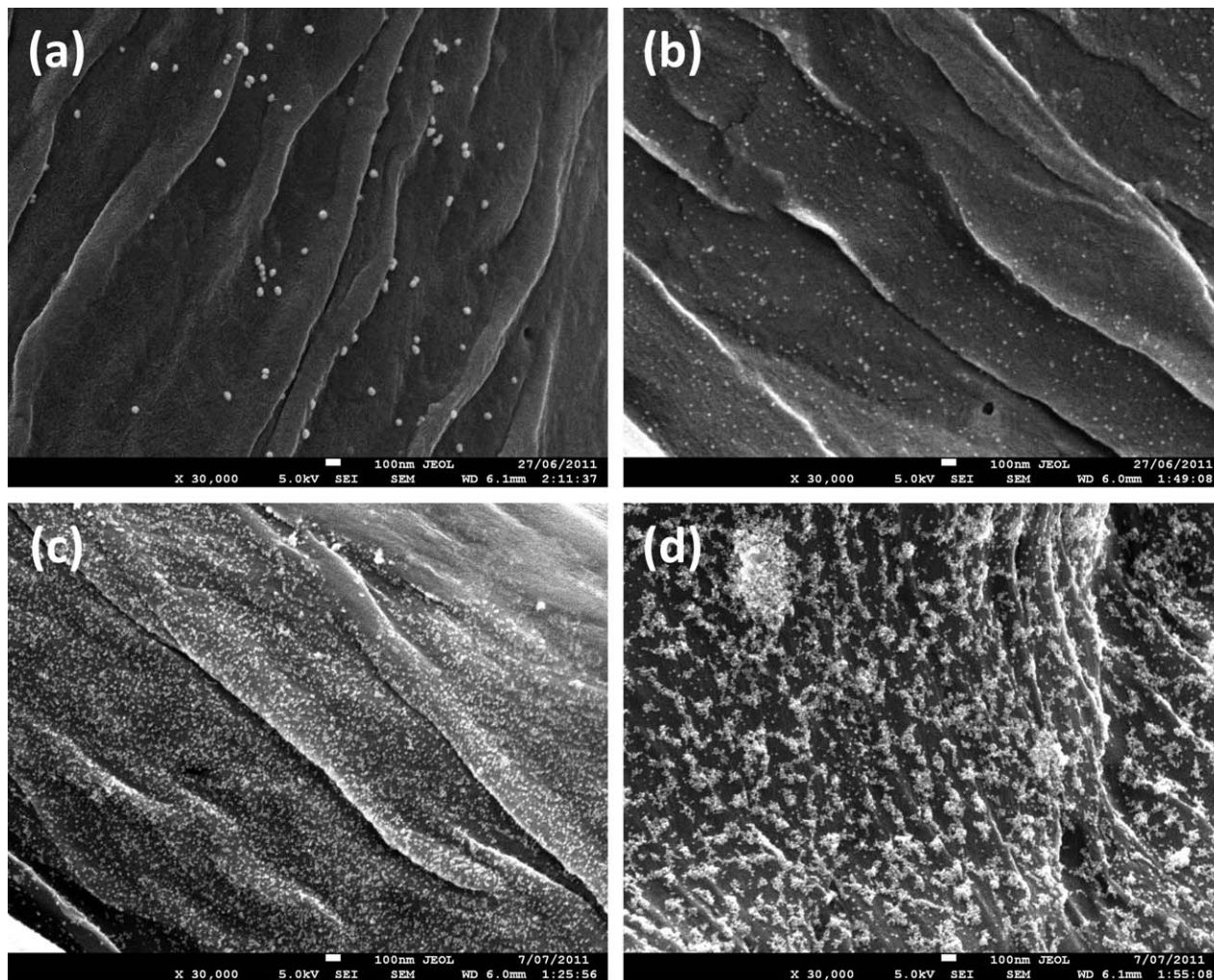


Figure 3. FESEM image of (a) 40 nm, (b) 20 nm, (c) concentrated 20 nm AuNPs on cotton thread, and (d) 20 nm concentrated AuNPs on CPAM pretreated cotton thread.

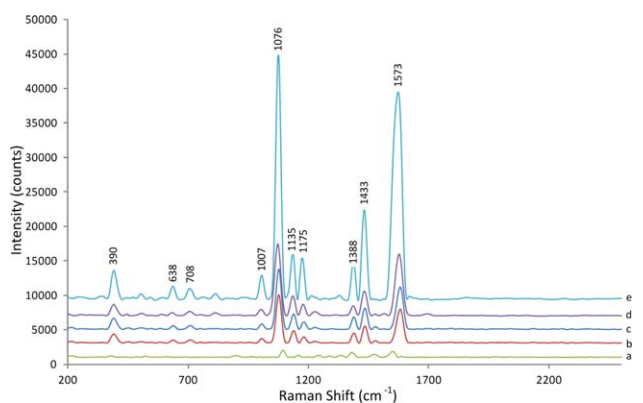


Figure 4. Comparison of Raman Spectra for 1mM 4-ATP on cotton threads coated with varying sizes of AuNPs and with or without CPAM.

(a) untreated thread, (b) 40 nm AuNPs, (c) 20 nm AuNPs, (d) concentrated 20 nm AuNPs, and (e) concentrated 20 nm AuNPs and CPAM. [Color figure can be viewed in the online issue, which is available at [wileyonlinelibrary.com](http://wileyonlinelibrary.com).]

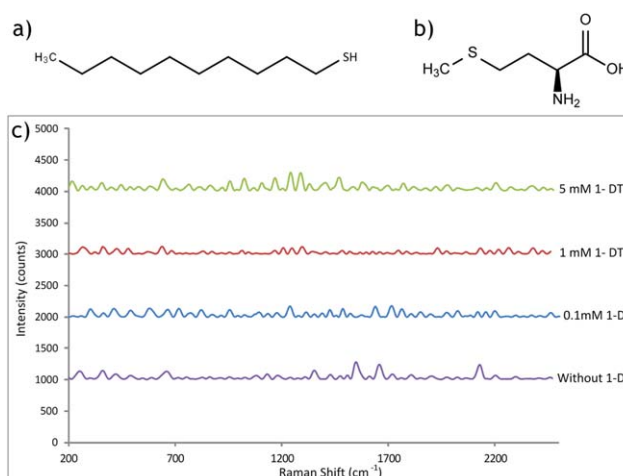
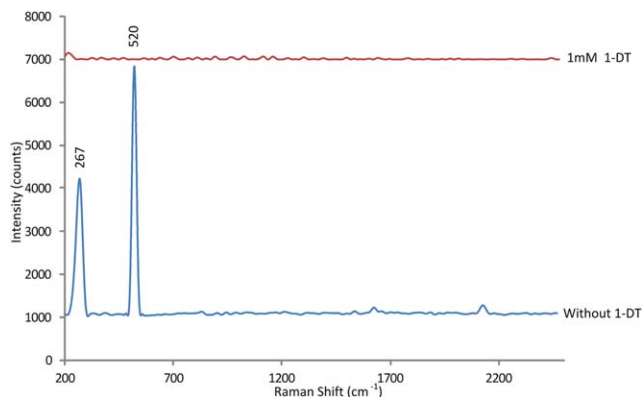


Figure 5. (a) Molecular structure of 1-DT, (b) Molecular structure of LM, and (c) SERS spectra of 1-DT at varying concentrations on AuNP-CPAM treated thread (0, 0.1mM, 1mM, and 5mM).

[Color figure can be viewed in the online issue, which is available at [wileyonlinelibrary.com](http://wileyonlinelibrary.com).]



**Figure 6. SERS spectra of AuNPs-CPAM treated silicon wafer without 1-DT and with 1 mM of 1-DT.**

[Color figure can be viewed in the online issue, which is available at [wileyonlinelibrary.com](http://wileyonlinelibrary.com).]

show a difference compared to the SERS spectrum of AuNPs treated silicon without 1-DT. The Raman peak for silicon at  $520.5\text{ cm}^{-1}$  is absent, when 1-DT was deposited on the silicon substrate. This could be due to the background signal from 1-DT which overcomes the signal from the silicon substrate. The spectrum of 1-DT does not show the characteristic peaks and is similar to those that are obtained from the thread substrates (Figure 5c). It is well known that thiol molecules can easily form a self-assembled monolayer on AuNPs through the strong S—Au bond.<sup>25–28</sup> The sulphide group is also highly reactive to gold<sup>29</sup>; it is therefore, expected that LM will also chemically bond to the AuNP surface. Our results for 1-DT and LM, therefore, suggest that other factors are at play which prevent the enhancement of the Raman signals for these particular analytes.

Raman spectroscopy (and therefore, SERS) measures the wavelength and intensity of light scattered from a molecule due to the excitation of the molecular vibration modes of chemical bonds. The intensity of Raman scattering  $I_R$  is given by

$$I_R \propto \nu^4 I_0 N \left( \frac{\Delta\alpha}{\Delta Q} \right)^2 \quad (1)$$

where  $I_0$  is the incident laser intensity,  $N$  is the number of scattering molecules in a given state,  $\nu$  is the exciting laser frequency,  $\alpha$  is the polarizability of the molecules, and  $Q$  is the vibrational amplitude.<sup>30</sup> It is therefore, follows that only molecular vibrations which cause a change in polarizability ( $\Delta\alpha$ ) are Raman active. Polarizability describes the deformability of the electron cloud about a molecule by an external electric field, and is strongly influenced by how tightly the electrons are bound to the nuclei. The absence of SERS signals from the adsorbed 1-DT and LM on AuNPs could be due to the lack of significant changes in polarizability of these molecules by the plasmonic effect of AuNPs. The main molecular structure of 1-DT is a straight aliphatic chain consisting of saturated sigma C—C and C—H bonds. The large number of covalent bonds gives the saturated aliphatic structure a relatively high polarizability; this property could be understood by considering the high polarizability of alkanes.<sup>31</sup> However, the highly localized bonding electrons of the covalent bonds in the molecule do not provide the saturated structures with the possibility of large changes in polarizability when excited by the plasmon at the surface of AuNPs, as the electrons are restricted in between the two

bonding atoms. A secondary reason is that the localized valence electrons of C—H bonds may not be effectively excited by the enhanced electromagnetic field at the surface of AuNPs. Normal alkyl thiols tend to form self-assembled layers, with the alkyl chains oriented at an angle near  $30^\circ$  away from the surface normal (i.e., direction perpendicular to the surface).<sup>32</sup> In this self-assembled molecular layer the H—C—H bonding planes of the alkyl chain are  $60^\circ$  away from the surface normal of AuNPs (which is also the direction of the plasmonic electric field in the hot spots). As hot spots in the plasmonic electric field induces the bond vibration most effectively when the bond orientation is parallel to the direction of the field, molecular bonds that are strongly off-parallel will not be effectively excited. Therefore, all vibration modes within the H—C—H bond plane of 1-DT (i.e., stretching and bending) would be further reduced.

Compared to 1-DT and LM which are molecules dominated by highly localized sigma bonds, 4-ATP consists of a benzene ring; its six  $\pi$  electrons are delocalized and form a conjugated  $\pi$ -bond with the amine group in the fourth position. The electrons in conjugated  $\pi$ -bonds are more easily displaced from their equilibrium positions by an external electric field. This could lead to a large change in molecular polarizability when excited by electric fields in hotspots. Besides, the adsorbed 4-ATP molecules also form self-assembled layers on metal surfaces. The molecular orientation of 4-ATP in the self-assembled layer has a small angle from the metal surface normal; thus, the molecular orientation strongly favors all the in-plane vibration modes. Therefore, 4-ATP shows a more intense result during SERS and almost all vibrational modes shown in Figure 2 are in-plane modes.<sup>18</sup> This effect explains why the presence of CPAM on the threads does not have a significant impact on the Raman spectra generated. CPAM (Figure 7) has a saturated hydrocarbon backbone and the molecular structure is dominated by localized covalent sigma bonds, and this explains how it can have such a negligible effect on the SERS signal despite being directly adjacent to the AuNPs.

Our results show that SERS is likely to be more useful for analysing molecules that have aromatic structures and delocalized valence electrons. Almost all articles in the literature on SERS have reported high Raman enhancement of molecules with such structures.<sup>33–36</sup>

### Unbound analyte testing

The traditional SERS model suggests that analyte molecules should be chemically bound to nanoparticle surfaces for signal enhancement to be achieved. While it is true that analyte molecules must be located within the enhanced

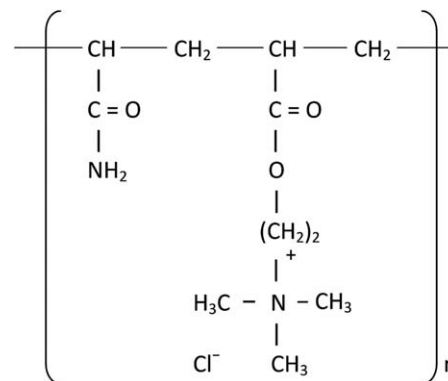


**Figure 7. Molecular structure of CPAM.**

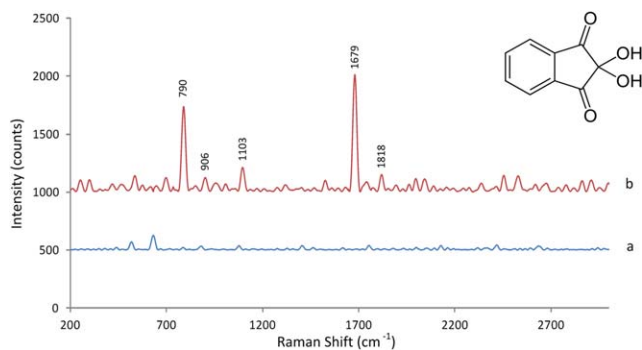


**Figure 8. (a) Raman spectrum of 1mM Ninhydrin (with molecular structure overlaid) on plain thread and (b) SERS spectrum of 1mM Ninhydrin on of AuNP-CPAM treated thread.**

[Color figure can be viewed in the online issue, which is available at [wileyonlinelibrary.com](http://wileyonlinelibrary.com).]

“hotspots” between adjacent nanoparticle clusters to achieve stronger Raman signal enhancement, this study investigated whether or not it was necessary for them to be strongly chemically bound to the nanoparticle surfaces. The three test molecules used in the proof of concept study, 1-DT, LM, and 4-ATP, all possess strong gold-binding thiol or thioether groups. The presence of this functional group ensures that these molecules will be chemically bound to the surface of the AuNPs. To evaluate whether this was necessary for achieving enhancement or not, testing of analytes which do not possess the thiol or thioether group or any other strongly gold-binding groups was required. Ninhydrin reagent and phenolphthalein (structures shown in Figures 8 and 9) were selected for this purpose as their structures not only lack any strongly gold-binding groups but also contain benzene rings which were expected to produce easily visible Raman signals. SERS analysis of the two analytes was performed on both plain, untreated thread and on thread treated with AuNPs. Figure 8 shows the combined spectra from the SERS analysis of ninhydrin ( $\nu(\text{C}-\text{C})$  aromatic ring vibration at  $790\text{cm}^{-1}$  and  $906\text{cm}^{-1}$ ,  $\delta(\text{CH})_{\text{Ph}}$   $1103\text{cm}^{-1}$ ,  $\nu(\text{C}=\text{O})$   $1679\text{cm}^{-1}$  and  $1818\text{cm}^{-1}$ ),<sup>30</sup> clearly displaying an enhancement due to the AuNPs on the thread substrate. This result is mirrored in the spectra of phenolphthalein ( $\nu(\text{CC})$  aromatic ring vibration at 411 and 468,  $\nu(\text{C}-\text{O}-\text{C})$  at  $830\text{cm}^{-1}$ ,  $\nu(\text{C}-\text{O})$  at  $1016\text{cm}^{-1}$ ,  $\delta(\text{CH})_{\text{Ph}}$  at  $1163\text{cm}^{-1}$ ,  $\nu(\text{C}=\text{C})$  and

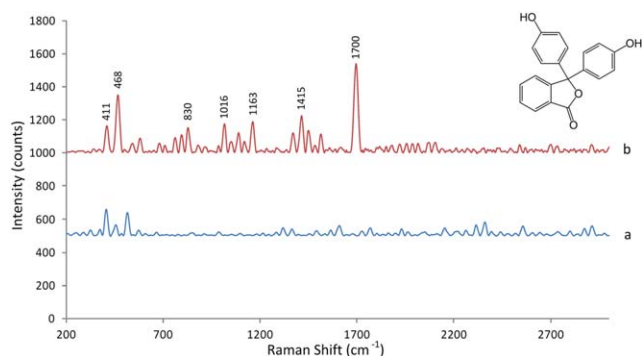


**Figure 9. (a) Raman spectra of 1mM of Phenolphthalein (with molecular structure overlaid) on plain thread and (b) on AuNP-CPAM treated thread.**

[Color figure can be viewed in the online issue, which is available at [wileyonlinelibrary.com](http://wileyonlinelibrary.com).]

$\delta(\text{OH})$  at  $1415\text{cm}^{-1}$ ,  $\nu(\text{C}=\text{O})$  at  $1700\text{cm}^{-1}$ )<sup>30,37,38</sup> in Figure 9 with a significant increase in the height of the signal peaks due to the presence of the AuNPs. These results strongly suggest that the enhancement effect of SERS is not entirely dependent on whether the analyte molecules are chemically bound to the AuNPs. It is instead likely that weaker forces of attraction are at work and acting to position analyte molecules within the hotspot enhancement regions, such as van der Waal's forces, for example. These weaker forces result in analyte molecules being located further away from the hotspots compared to those which can chemically bind, and therefore, lower signal intensity was observed. Despite this, unbound molecules still achieved sufficient enhancement to allow their identification by SERS.

## Conclusions

This study shows the viable potential of AuNP-functionalized thread substrates to be used and optimized as disposable, low-cost-per-test diagnostics, for routine SERS spectroscopy. The threads used were inexpensive and required only small volumes of both sample solution and treatment solution to produce strong results, an inherent advantage over alternatives such as paper. The low volume requirement for AuNP treatment solution coupled with the almost insignificant cost of a small piece of cotton thread mean that despite the high fixed costs of the SERS equipment, the cost per test using this platform is extremely low. The flexibility of the platform was illustrated by the varied range of analytes that were successfully tested. Overall, a novel, low-cost platform for SERS analysis has been developed which possesses several desirable advantages over contemporary alternatives.

This presents the first use of cotton thread as an efficient SERS active substrate for probing 4-ATP. By controlling the aggregation state of the AuNPs on thread using cationic polymer, greatly amplified SERS signals were achieved for a range of analytes. Additionally, this study also demonstrated that molecules with highly localized valence electrons and  $\sigma$ -bonds receive much lower signal enhancement from SERS as the change in polarizability of such analyte molecules by the enhancing plasmonic electric field is limited for these analytes. It was observed that SERS analysis was effective for detecting certain types of analyte molecules such as those which possess aromatic structures with delocalized valence electrons. Molecules with delocalized  $\pi$ -bonds may have greater changes in polarizability when excited by the plasmonic electric field. This study experimentally observed that 1-DT, LM and CPAM, which have the main molecular structure of saturated C-C and C-H  $\sigma$ -bonds, display little Raman activity. This may be related to the fact that bonding electrons in those molecules are highly localized and have weak changes in polarizability when interacting with the plasmonic electric field.

This study illustrated that analytes do not have to be chemically bound to the surface of the Au-NPs to generate an enhancement of Raman signal. Analyte molecules which lack gold-binding functional groups but are able to acquire big changes in polarizability, when excited in the hotspots are still subject to signal enhancement. It was observed that the structure of the analyte molecules played a significant role in the level of SERS signal achieved, and as a result the technique is limited to the detection of only a small number of analytes, which possess highly polarizable molecule structure.

## Acknowledgments

This work is supported by the Australian Research Council Grant (ARC DP1094179 and ARC LP0990526), as well as grants from the Thailand Research Fund (TRF) through the Royal Golden Jubilee PhD Program (RGJ) and the Center of Excellence for Innovation in Chemistry (PERCH-CIC), Commission on Higher Education, Ministry of Education. The authors would like to thank Dr. Tim Williams and Finlay Shanks, Monash University for technical expertise and AQUA + TECH for supplying the CPAM polymers (Snow-Flake Cationics). The authors also thank Dr. Lijing Wang of the School of Fashion and Textiles, RMIT University, for kindly providing thread and textile samples and Mr Hansen Shen, student of the Faculty of Law of Monash University for proof reading the manuscript. Author Purim Jarujamrus also extends his thanks to his former supervisors Prof. Juwadee Shiowatana & Assistant Prof. Atitaya Siripinyanond, and research team at the Department of Chemistry and Center for Innovation in Chemistry, Faculty of Science, Mahidol University, Thailand. The research scholarships of Monash University and the Department of Chemical Engineering are also gratefully acknowledged.

## Literature Cited

1. Kaminska A, Inya-Agha O, Forster RJ, Keyes TE. Chemically bound gold nanoparticle arrays on silicon: assembly, properties and SERS study of protein interactions. *Phys Chem Chem Phys*. 2008;10(28):4172–4180.
2. Jackson JB, Halas NJ. Surface-enhanced Raman scattering on tunable plasmonic nanoparticle substrates. *Proc Natl Acad Sci USA*. 2004;101(52):17930–17935.
3. Luo L-B, Chen L-M, Zhang M-L, He Z-B, Zhang W-F, Yuan G-D, Zhang W-J, Lee S-T. Surface-enhanced Raman scattering from uniform gold and silver nanoparticle-coated substrates. *J Phys Chem C*. 2009;113(21):9191–9196.
4. Petlicki J, van de Ven TGM. Adsorption of polyethylenimine onto cellulose fibers. *Colloids Surf A*. 1994;83(1):9–23.
5. Bizzarri MSPAR, Cannistraro MSPS. SERS detection of thrombin by protein recognition using functionalized gold nanoparticles. *Nano-medicine*. 2007;3(4):306–310.
6. Hesse E, Creighton JA. Investigation of cyanide ions adsorbed on platinum and palladium coated silver island films by surface-enhanced Raman spectroscopy. *Chem Phys Lett* 1999;303(1–2):101–106.
7. Chen Y-H, Yeh C-S. Laser ablation method: use of surfactants to form the dispersed Ag nanoparticles. *Colloids Surf A*. 2002;197(1–3):133–139.
8. Ngo YH, Li D, Simon GP, Garnier G. Gold Nanoparticle–paper as a three-dimensional surface enhanced Raman scattering substrate. *Langmuir*. 2012;28(23):8782–8790.
9. Ngo YH, Li D, Simon GP, Garnier G. Effect of cationic polyacrylamides on the aggregation and SERS performance of gold nanoparticles-treated paper. *J Colloid Interface Sci*. 2013;392:237–246.
10. Ngo YH, Li D, Simon GP, Garnier G. Paper surfaces functionalized by nanoparticles. *Adv Colloid Interface Sci*. 2011;163(1):23–38.
11. Li X, Tian J, Shen W. Thread as a versatile material for low-cost microfluidic diagnostics. *ACS Appl Mater Interfaces*. 2009;2(1):1–6.
12. Ballerini D, Li X, Shen W. An inexpensive thread-based system for simple and rapid blood grouping. *Anal Bioanal Chem*. 2011;399(5):1869–1875.
13. Ballerini DR, Li X, Shen W. Flow control concepts for thread-based microfluidic devices. *Biomicrofluidics*. 2011;5:14105–14105.
14. Li X, Tian J, Garnier G, Shen W. Fabrication of paper-based microfluidic sensors by printing. *Colloids Surf B*. 2010;76(2):564–570.
15. Turkevich J, Stevenson PC, Hillier J. A study of the nucleation and growth processes in the synthesis of colloidal gold. *Discuss Faraday Soc*. 1951;11:55–75.
16. Cadotte M, Tellier M-E, Blanco A, Fuente E, van de Ven TGM, Paris J. Flocculation, retention and drainage in papermaking: a comparative study of polymeric additives. *Can J Chem Eng*. 2007;85(2):240–248.

17. Li X, Ballerini D, Tian J, Shen W. Thread as a substrate for low-cost point-of-care diagnostics. *Sustainable Chemistry*, 2011. WIT Press, 2011.
18. Hu X, Wang T, Wang L, Dong S. Surface-enhanced Raman scattering of 4-aminothiophenol self-assembled monolayers in sandwich structure with nanoparticle shape dependence: off-surface plasmon resonance condition. *J Phys Chem C*. 2007;111(19):6962–6969.
19. Ko H, Singamaneni S, Tsukruk VV. Nanostructured surfaces and assemblies as SERS media. *Small*. 2008;4(10):1576–1599.
20. Abe K, Suzuki K, Citterio D. Inkjet-printed microfluidic multianalyte chemical sensing paper. *Anal Chem*. 2008;80(18):6928–6934.
21. Toderas F, Baia M, Baia L, Astilean S. Controlling gold nanoparticle assemblies for efficient surface-enhanced Raman scattering and localized surface plasmon resonance sensors. *Nanotechnology*. 2007;18:255702.
22. Michaels AM, Jiang J, Brus L. Ag nanocrystal junctions as the site for surface-enhanced Raman scattering of single rhodamine 6G molecules. *J Phys Chem B*. 2000;104(50):11965–11971.
23. Aponte MI. *Effect of Alkanethiol Self-Assembled Monolayers on the Plastic and Elastic Deformation of Gold(III) Films*. New Jersey: Materials Science and Engineering, The state University of New Jersey, 2010.
24. Graff M, Bukowska J. Surface-enhanced Raman scattering (SERS) spectroscopy of enantiomeric and racemic methionine on a silver electrode-evidence for chiral discrimination in interactions between adsorbed molecules. *Chem Phys Lett*. 2011;509(1–3):58–61.
25. Vericat C, Vela ME, Salvarezza RC. Self-assembled monolayers of alkanethiols on Au(111): surface structures, defects and dynamics. *Phys Chem Chem Phys*. 2005;7(18):3258–3268.
26. Bisio F, Prato M, Barborini E, Canepa M. Interaction of alkanethiols with nanoporous cluster-assembled Au films. *Langmuir*. 2011;27(13):8371–8376.
27. Shalom D, Wootton RCR, Winkle RF, Cottam BF, Vilar R, deMello AJ, Wilde CP. Synthesis of thiol functionalized gold nanoparticles using a continuous flow microfluidic reactor. *Mater Lett*. 2007;61(4–5):1146–1150.
28. Jadzinsky PD, Calero G, Ackerson CJ, Bushnell DA, Kornberg RD. Structure of a thiol monolayer-protected gold nanoparticle at 1.1 Å resolution. *Science*. 2007;318(5849):430–433.
29. Lide DR, Beyer WH, Weast RC, Center UoRICR, Astle MJ. *CRC Handbook of Chemistry and Physics: A Ready-reference Book of Chemical and Physical Data*. Boca Raton FLA, USA: CRC Press, 1987.
30. Larkin P. *Infrared and Raman Spectroscopy*. Waltham, MA, USA: Elsevier, 2011.
31. Bellisario DO, Jewell AD, Tierney HL, Baber AE, Sykes ECH. Adsorption, assembly, and dynamics of dibutyl sulfide on Au{111}. *J Phys Chem C*. 2010;114(34):14583–14589.
32. Love JC, Estroff LA, Kriebel JK, Nuzzo RG, Whitesides GM. Self-assembled monolayers of thiolates on metals as a form of nanotechnology. *Chem Rev (Washington, DC, U.S.)*. 2005;105(4):1103–1170.
33. Kim K, Yoon JK. Raman scattering of 4-aminobenzenethiol sandwiched between Ag/Au nanoparticle and macroscopically smooth Au substrate. *J Phys Chem B*. 2005;109(44):20731–20736.
34. Hu X, Cheng W, Wang T, Wang Y, Wang E, Dong S. Fabrication, characterization, and application in SERS of self-assembled polyelectrolyte-gold nanorod multilayered films. *J Phys Chem B*. 2005;109(41):19385–19389.
35. Osawa M, Matsuda N, Yoshii K, Uchida I. Charge transfer resonance Raman process in surface-enhanced Raman scattering from p-aminothiophenol adsorbed on silver: Herzberg-Teller contribution. *J Phys Chem*. 1994;98(48):12702–12707.
36. Sheng P, Wu S, Bao L, Wang X, Chen Z, Cai Q. Surface enhanced Raman scattering detecting polycyclic aromatic hydrocarbons with gold nanoparticle-modified TiO<sub>2</sub> nanotube arrays. *New J Chem*. 2012;36(12):2501–2505.
37. Kunimoto K-K, Sugiura H, Kato T, Senda H, Kuwae A, Hanai K. Molecular structure and vibrational spectra of phenolphthalein and its dianion. *Spectrochimica Acta Part A*. 2001;57(2):265–271.
38. Chattopadhyay S, Kastha GS, Nandy SK, Brahma SK. Resonance Raman spectrum of phenolphthalein in alkaline solution and vibrational spectra of the pure compound and its potassium salts. *J Raman Spectrosc*. 1989;20(10):651–654.

Manuscript received Mar. 18, 2013, and revision received Jan. 24, 2014.